Kinetic and Molecular Analysis of 5-Epiaristolochene 1,3-Dihydroxylase, a Cytochrome P450 Enzyme Catalyzing Successive Hydroxylations of Sesquiterpenes[*,S]

Shunji Takahashi[‡], **Yuxin Zhao[§]**, **Paul E. O'Maille[¶]**, **Bryan T. Greenhagen[‡]**, **Joseph P. Noel[¶]**, **Robert M. Coates[§]**, and **Joe Chappell[‡,||]**

[‡] Plant Physiology, Biochemistry, and Molecular Biology Program, Agronomy Department, University of Kentucky, Lexington, Kentucky, 40546-0312

[§] Department of Chemistry, University of Illinois, Urbana, Illinois 61801

[¶] Salk Institute for Biological Studies, La Jolla, California 92037

Abstract

The final step of capsidiol biosynthesis is catalyzed by 5-epiaristolochene dihydroxylase (EAH), a cytochrome P450 enzyme that catalyzes the regio- and stereospecific insertion of two hydroxyl moieties into the bicyclic sesquiterpene 5-epiaristolochene (EA). Detailed kinetic studies using EA and the two possible monohydroxylated intermediates demonstrated the release of 1β-hydroxy-EA ((OH)EA) at high EA concentrations and a 10-fold catalytic preference for 1β(OH)EA *versus* 3α(OH)EA, indicative of a preferred reaction order of hydroxylation at C-1, followed by that at C-3. Sequence alignments and homology modeling identified active-site residues tested for their contribution to substrate specificity and overall enzymatic activity. Mutants EAH-S368C and EAH-S368V exhibited wild-type catalytic efficiencies for 1β(OH)EA biosynthesis, but were devoid of the successive hydroxylation activity for capsidiol biosynthesis. In contrast to EAH-S368C, EAH-S368V catalyzed the relative equal biosynthesis of 1β(OH)EA, 2β(OH)EA, and 3β(OH)EA from EA with wild-type efficiency. Moreover, EAH-S368V converted ~1.5% of these monohydroxylated products to their respective ketone forms. Alanine and threonine mutations at position 368 were significantly compromised in their conversion rates of EA to capsidiol and correlated with 3.6- and 5.7-fold increases in their K_m values for the 1β(OH)EA intermediate, respectively. A role for Ile[486] in the successive hydroxylations of EA was also suggested by the EAH-I468A mutant, which produced significant amounts 1β(OH)EA, but negligible amounts of capsidiol from EA. The altered product profile of the EAH-I486A mutant correlated with a 3.6-fold higher K_m for EA and a 4.4-fold slower turnover rate (k_{cat}) for 1β(OH)EA. These kinetic and mutational studies were correlated with substrate docking predictions to suggest how Ser[368] and Ile[486] might contribute to active-site topology, substrate binding, and substrate presentation to the oxo-Fe-heme reaction center.

The mevalonate and methylerythritol phosphate pathways are responsible for the biosynthesis of isoprenoids, a diverse group of organic natural products found in animals, plants, fungi, insects, and bacteria. Isoprenoids are further divided into classes of primary

and secondary metabolites. Isoprenoids that are primary metabolites include sterols, carotenoids, hormones, and long chain hydrocarbons used to tether particular enzymes to membrane systems, compounds essential for viability. Isoprenoids classified as secondary metabolites include monoterpenes, sesquiterpenes, diterpenes, and triterpenes, and many of these mediate interactions between organisms and their environments (1–5).

Capsidiol is a bicyclic dihydroxylated sesquiterpene produced by several solanaceous plants in response to pathogen or elicitor challenge (6–10) and is considered an important plant defense response because it can prevent the germination and growth of several fungal species (11). Capsidiol biosynthesis is regulated by the expression of two key enzymes (see Scheme 1). 5-Epiaristolochene synthase catalyzes the cyclization of farnesyl diphosphate to the bicyclic intermediate 5-epiaristolochene (EA)[1,2] and is responsible for the diversion of farnesyl diphosphate from the mevalonate pathway toward antimicrobial compound biosynthesis (12,13). Recently, two highly homologous cDNAs for EA dihydroxylase (EAH) were isolated from *Nicotiana tabacum* and functionally expressed in yeast, and the encoded proteins were characterized as cytochrome P450 enzymes catalyzing the stereo- and regiospecific hydroxylation of EA at C-1 and C-3 (see Scheme 1) (14).

Plant P450 enzymes known to catalyze regiospecific monohydroxylation of carbocyclic structures include limonene 3- and 6-hydroxylases (15,16); cinnamate 4-hydroxylase (17); ferulate 5-hydroxylase (18,19); taxoid 10β-, 13α-, and 14β-hydroxylases (20–22); the CYP71C subfamily enzymes for 2,4-dihydroxy-7-methoxy-1,4-benzoxazin-3-one biosynthesis in maize and wheat (23,24); and members of the CYP90 family involved in the biosynthesis of the steroid hormone brassinolide (25,26). Successive hydroxylation/ oxidation reactions catalyzed by plant P450 enzymes have also been documented for tyrosine *n*-hydroxylase involved in the biosynthesis of the cyanogenic glucoside dhurrin (27), flavonoid 3′,5′-hydroxylase in anthocyanin biosynthesis (28,29), and several of the enzymes in the gibberellin biosynthetic pathway (30–33). For example, flavonoid 3′,5′-hydroxylase (28,29) catalyzes the planar insertion of hydroxyl groups into the equivalent *meta*-positions (C-3′ and C-5′) of the flavonoid B (phenolic) ring and yields 3′-, 5′-, and 3′, 5′-hydroxylated reaction products (29). *ent*-Kaurene oxidase (32) catalyzes the successive oxidation of the methyl substituent of *ent*-kaurene at C-19 en route to *ent*-kaurenoic acid. *ent*-Kaurenoic acid is itself subject to multiple oxidations and a ring contraction through the action of a single P450, CYP88A, or *ent*-kaurenoic acid oxidase (33). Interestingly, although flavonoid 3′, 5′-hydroxylase and both *ent*-kaurene and *ent*-kaurenoic acid oxidases catalyze regiospecific hydroxylations, these enzymes do not exhibit the regio- and stereospecific complexity of EAH. EAH introduces hydroxyl groups at distal sites on opposite faces of the epiaristolochene ring system (see Scheme 1).

A preferred order for the successive hydroxylation of EA has yet to be determined (see Scheme 1). Of the two possible monohydroxylated intermediates of EA, only 3α-hydroxy-EA (3α(OH)EA) has been reported as a minor metabolite accumulating in pepper fruits challenged with fungal spores (34), suggesting that small amounts of this reaction intermediate might be released as a general consequence of catalysis. Consistent with this notion are several observations that 3α(OH)EA can be converted to capsidiol. Whitehead *et al.* (35) reported a modest conversion of 3α(OH)EA to capsidiol when radiolabeled forms of this intermediate were fed to either control or elicitor-treated callus cultures of tobacco.

---

[1]The abbreviations used are: EA, 5-epiaristolochene; EAH, 5-epiaristolochene dihydroxylase; (OH)EA, hydroxy-5-epiaristolochene; GC/MS, gas chromatography/mass spectrometry; CHAPS, 3-[(3-cholamidopropyl)dimethylammonio]-1-propanesulfonic acid; SRS, substrate recognition site.
[2]The proper semi-systematic name for 5-epiaristolochene is 4-*epi*-eremophila-1(10),11(12)-diene. The common name 5-epiaristolochene relating the structure to (−)-aristolochene (4,5-di-*epi*-eremophila-9(10),11(12)-diene) is widely used in the literature and is adopted in this work for that reason.

However, although Ralston *et al.* (14) documented the ready conversion of 3α(OH)EA to capsidiol by microsomes from yeast overexpressing the EAH gene, they also reported the biosynthesis of capsidiol without the accumulation of either monohydroxylated intermediate, 3α(OH)EA or 1β(OH)EA, in reactions incubated with low concentrations (<1 μM) of the EA substrate. Although 1β(OH)EA has not been reported as a reaction product of EAH or observed in plants exposed to exogenous stimuli, preference for P450-mediated hydroxylations of mono- and diterpenes occurring allylic to carbon–carbon double bonds (16,20,21) suggests that the initial hydroxylation catalyzed by EAH could occur at C-1, followed by that at C-3.

This work describes investigations of the successive regio-and stereospecific hydroxylation of EA by EAH. The ready availability of EA, 3α(OH)EA, and 1β(OH)EA greatly facilitated our ability to perform detailed kinetic studies to address the preferred order of hydroxylation. Sequence comparisons with related P450 enzymes and modeling of EAH based upon the mammalian 2C5 steroid hydroxylase structure (36) enabled us to identify amino acid residues potentially providing catalytic specificity to these reactions. These structural hypotheses were then tested by site-directed mutagenesis and kinetic analysis. Together, the results demonstrate a preferred reaction order and provide evidence that Ser[368] and Ile[486] play a significant role in orchestrating the successive hydroxylation of EA to capsidiol.

EXPERIMENTAL PROCEDURES

Chemicals

Standard laboratory reagents were purchased from Fisher, Sigma, and Aldrich. Authentic standards of EA, 3α(OH)EA, and capsidiol were available from previous work (14). Synthesis of 1β(OH)EA, 3β(OH)EA, EA-1-one, and EA-3-one was conducted as described (37).

Site-directed Mutagenesis

All mutations were engineered into the CYP71D20 (EAH) cDNA using the standard QuikChange protocol (Stratagene) (38). A full-length EAH cDNA (GenBank[TM]/EBI accession number AF368376) inserted into the BamHI/EcoRI restriction sites of the pBluescript II KS(+) vector was used in combination with *Pfu*Turbo DNA polymerase (Stratagene) and the following primer pairs (with the mutation sites underlined): S368A primers, 5′-GACTTCATCCACCGGCTCCACTTTTGGTCC-3′ and 5′-GGACCAAAAGTGGAGCCGGTGGATGAAGTC-3′; S368C primers, 5′-GACTTCATCCACCGTGTCCACTTTTGGTCC-3′ and 5′-GGACCAAAAGTGGACACGGTGGATGAAGTC-3′; S368T primers, 5′-GACTTCATCCACCGACTCCACTTTTGGTCC-3′ and 5′-GGACCAAAAGTGGAGTCGGTGGATGAAGTC-3′; S368V primers, 5′-GACTTCATCCACCGGTTCCACTTTTGGTCC-3′ and 5′-GGACCAAAAGTGGAACCGGTGGATGAAGTC-3′; S368I primers, 5′-GACTTCATCCACCGATTCCACTTTTGGTCC-3′ and 5′-GGACCAAAAGTGGAATCGGTGGATGAAGTC-3′; S368F primers, 5′-GACTTCATCCACCGTTTCCACTTTTGGTCC-3′ and 5′-GGACCAAAAGTGGAAACGGTGGATGAAGTC-3′; I486A primers, 5′-CGAATTATCGGGAATAACTGCTGCTAGAAAGGGTGGCC-3′ and 5′-GGCCACCCTTTCTAGCAGCAGTTATTCCCGATAATTCG-3′. Site-specific mutations were confirmed by automated DNA sequencing performed using the Big-Dye Terminator Cycle sequencing protocol of PerkinElmer Life Sciences in combination with an ABI Prism 310 genetic analyzer (Applied Biosystems, Foster City, CA). Mutated cDNAs were

subsequently subcloned from the pBluescript vector into the corresponding BamHI/EcoRI sites of pYeDP60, a standard yeast expression vector providing galactose inducibility for expression of the inserted cDNA (39).

Yeast Expression and Microsome Preparations

Expression vectors harboring wild-type or mutant EAH were introduced into the WAT11 yeast strain, a strain previously engineered with an *Arabidopsis* NADPH-cytochrome P450 reductase gene (40) and kindly provided by Dr. P. Urban (Centre de Génétique Moléculaire, CNRS, Gif-sur-Yvette, France). Transformants were grown from single colonies; expression of the EAH cDNAs was induced by galactose addition to the growth medium; and microsomes were prepared as described previously (41).

CO Difference Spectra

CO difference spectra were determined to estimate the amount of properly folded wild-type and mutant EAH proteins in microsome preparations. The amount of functional P450 was calculated using an extinction coefficient of 91 mM^{-1} cm^{-1} at 450 nm (42). The wild-type and mutant enzymes showed a clear absorption maximum at 450 nm (Supplemental Fig. 1), consistent with properly folded enzymes having the heme cofactor oriented in the correct electron spin state.

EAH Assays

Standard assays were performed in 1-ml glass vials with a final reaction volume of 200 μl containing 4% Me$_2$SO, 2.4 mM NADPH, 100 mM Tris-HCl (pH 7.5), and microsomes at a final concentration of 90 or 180 pmol of EAH protein eq (determined by CO difference spectroscopy)/ml. Substrate concentrations were varied from 2 to 100 μM for EA, 3 to 30 μM for 3α(OH)EA, and 0.5 to 30 μM for 1β(OH)EA. After preincubation of the reaction mixtures at 30 °C for 5 min, the reactions were initiated by the addition of 2.4 mM NADPH and allowed to proceed for 2 min (EA), 1 min (1β(OH)EA), or 5 min (3α(OH)EA), which allowed for 5–20% conversion of substrate to reaction product(s). The reactions were terminated by the rapid addition of 400 μl of ethyl acetate and mixed by vortexing, followed by removal of the ethyl acetate extract. A second ethyl acetate extract was combined with the first, and the combined organic extracts were carefully concentrated on ice under N$_2$ gas, redissolved in 20 μl of ethyl acetate containing 10 ng/μl valencene as an internal standard, and subjected to gas chromatography (GC) and GC/mass spectrometry (MS) analyses. Assays were performed in triplicate for each substrate concentration, and kinetic constants were calculated by a nonlinear regression fit to the Michaelis-Menten equation using EnzymeKinetics Version 1.5 software (Trinity Software). Kinetic constants calculated from Lineweaver-Burk, Eadie-Hofstee, and Hanes-Woolf plots were not significantly different from those derived from nonlinear regression. Optimized reactions were linear with respect to reaction product generation over time and corresponded to a 5–20% conversion of substrate to product, sufficient to generate 1 ng or more of reaction product(s) readily quantified and identifiable by GC/MS.

Reaction Product Analyses

Quantification of the reaction products as well as standards of EA, 1β(OH)EA, 3α(OH)EA, and capsidiol was routinely performed using (+)-valencene (Fluka, Buchs, Switzerland) as an internal standard. Accuracy of the valencene standard was periodically verified relative to a (−)-α-cedrene standard (Fluka). Reaction products (1-μl aliquots) were quantified with an HP-5890 gas chromatograph equipped with an HP-5 capillary column (30 m × 0.25 mm, 0.25-μm phase thickness) and a flame ionization detector as described previously (38). Splitless injections were performed at an injection port temperature of 250 °C with an initial

column temperature of 140 °C maintained for 0.5 min. The column temperature was then increased to 230 °C with a 4 °C/min gradient. In addition to comigration and retention time comparisons with authentic standards, reaction products were identified by MS using a Thermo Finnigan DSQ GC/MS system equipped with a Restec Rtx-5 capillary column (30 m × 0.32 mm, 0.25-μm phase thickness). Samples were injected in the splitless mode at 250 °C with an initial oven temperature of 70 °C for 1 min, followed by an 8 °C/min gradient to 230 °C. Mass spectra were recorded at 70 eV, scanning from 35 to 300 atomic mass units, and compared with authentic standards for verification.

Purification of the EAH-S368V Reaction Products

To isolate and identify the EAH-S368V reaction products, ethyl acetate extracts from the *in vitro* assays were carefully concentrated under an N_2 stream and resuspended with hexane such that the final ethyl acetate concentration was <2%. The sample was then applied to a 230–400 mesh silica column (0.5 × 1 cm), and the hydrocarbon fraction was collected with a 2-ml hexane wash. Hydroxylated products were selectively eluted with 2 ml of a 1:19 (v/v) ethyl acetate/hexane solution, followed by 2 ml of a 1:4 (v/v) ethyl acetate/hexane solution. The fractions were carefully reconcentrated under an N_2 stream before GC/MS analysis.

Computational Studies

Homology modeling was performed with Modeler Version 6.2 (43–45) by threading the EAH amino acid sequence (GenBank[TM]/EBI accession number AF368376) onto the structural coordinates for the mammalian P450 2C5 protein (Protein Data Bank code 1DT6) (36). Ligands EA, 1β(OH)EA, and 3α(OH)EA were created using Chemdraw Ultra Version 7.0.1, energy-minimized with MOPAC in Chem3D Ultra Version 7.0 (CambridgeSoft Corp., Cambridge, MA), and subsequently used in docking simulation experiments. Docking calculations were conducted with GOLD Version 1.2 software (Genetic Optimization for Ligand Docking, Cambridge Crystallographic Data Centre, Cambridge, United Kingdom) (46–49).

RESULTS

Optimization of the EAH Activity

Numerous preliminary experiments were performed to optimize EAH activity for the conversion of EA to capsidiol. For example, the ability of a miscible organic co-solvent and various detergents to improve EA solubility was assessed. Maximum conversion of EA to capsidiol activity was observed at final concentrations of 2–5% (v/v) Me_2SO, but was inhibited at concentrations >10%. Detergents were also evaluated at concentrations ranging from 0.01 to 0.1%. Triton X-100 (v/v), deoxycholate (w/v), and 1-*O*-octyl β-D-glucopyranoside (w/v) all inhibited EAH activity, whereas CHAPS (w/v) and Tween 20 (v/v) had no effect. Standard assays were therefore performed using EA stock solutions dissolved in Me_2SO and assayed at a final Me_2SO concentration of 4% (v/v) in all reaction assays. The pH optimum was determined using 100 mM Tris-HCl (pH 7.2–9.2) and phosphate (pH 6.0–7.5) buffering systems. Maximum activity was observed at pH 7.5 with little preference for either the Tris-HCl or phosphate buffer. The optimum NADPH concentration for EAH activity was also determined. The maximum conversion rate for EA to capsidiol was observed at 0.3 mM and remained saturated up to a final concentration of 2.4 mM. The K_m for NADPH was subsequently estimated to be 61 ± 5 μM. All subsequent enzyme assays were therefore performed at optimized reaction conditions of 4% (v/v) Me_2SO and 2.4 mM NADPH in 100 mM Tris-HCl (pH 7.5).

Kinetic Analysis of EAH Indicates a Specific Reaction Order

To initially address the hydroxylation specificity of EAH (Scheme 1), we tested the enzyme for substrate preference for either of the putative reaction intermediates, 3α(OH)EA and 1β(OH)EA (Fig. 1). Microsomes from WAT11 yeast overexpressing the EAH gene were used as the enzyme source, and the absolute amount of active EAH enzyme was calculated from the carbon monoxide difference spectra. Both 3α(OH)EA and 1β(OH)EA were converted to capsidiol by EAH in NADPH-dependent reactions, but with different efficiencies. The K_m for 1β(OH)EA was ~4 times lower and the k_{cat} was ~3 times higher than those for 3α(OH)EA, resulting in a catalytic efficiency (k_{cat}/K_m) for 1β(OH)EA ~10 times greater than that for 3α(OH)EA (Table I). The kinetic constants for the hydrocarbon substrate EA were also determined (Fig. 2 and Table I). Although the K_m for the hydrocarbon substrate was considerably higher than that for either of the monohydroxylated intermediates, the turnover rates for EA and 1β(OH)EA were similar and significantly greater than that for 3α(OH)EA.

The kinetic constants reported in Table I are consistent with a catalytic barrier to the successive hydroxylation of the 3α(OH)EA intermediate and suggested that 1β(OH)EA would be the preferred monohydroxylated intermediate. In an effort to capture the release of an initial reaction intermediate, assays were performed with increasing concentrations of EA (2–100 μM), and the reaction product profiles were determined (Fig. 2). Reaction products were observed only after incubations with NADPH and were identified by GC/MS comparisons with authentic standards (Fig. 3). Capsidiol production reached a maximum at ~40 μM EA and gradually decreased after that. Although no monohydroxylated intermediates were detectable at EA concentrations below 16 μM, a proportionate increase in the biosynthesis of 1β(OH)EA was observed at EA concentrations above 20 μM. In contrast, no release of 3α(OH)EA was observed over the entire concentration range investigated.

Molecular Analysis of the Dihydroxylase Activities

A combination of computational methods was used to identify structural elements possibly contributing to the successive hydroxylation activity of EAH (Fig. 4). Sequence alignment of EAH with the known substrate recognition sites (SRSs) of closely related P450 enzymes of the CYP71D subfamily (50) revealed several potentially important sites. SRS-5 and SRS-6 were of particular interest given their proximity to the active site in several P450 structures (51) and because specific amino acid positions within these regions have previously been correlated with regio- and stereospecific reaction mechanisms (Fig. 4A) (52–61). A homology model of EAH derived from comparison with the mammalian CYP2C5 structure was constructed (Fig. 4B), and the resultant model suggested that Ser[368] and Ile[486] project into the active-site cavity oriented toward the heme catalytic site (Fig. 4C).

To investigate the contributions, if any, of Ser[368] and Ile[486] to either the first or second hydroxylation reaction as predicted by computational studies, site-specific mutations were generated at each position. The mutant genes were expressed in WAT11 yeast lines, and the absolute amount of newly synthesized microsomal enzyme was calculated from the carbon monoxide difference spectra (Supplemental Fig. 1). Mutant enzymes were then examined for substrate preferences and product specificity by steady-state kinetic analyses (Fig. 5 and Table II). Mutant enzymes harboring smaller amino acid substitutions such as Ala, Thr, Cys, and Val demonstrated reasonable CO binding spectra and were catalytically active. EAH-S368A and EAH-S368T retained their ability to fully convert EA to capsidiol, but the turnover rates for capsidiol formation were 3–13 times lower compared with that of the wild-type enzyme. EAH-S368A and EAH-S368T were also able to convert 1β(OH)EA to capsidiol with k_{cat} values comparable with that of wild-type EAH, but with K_m values for

1β(OH)EA 4–6 times greater compared with that of wild-type EAH. Although mutant enzymes containing bulky amino acid substitutions such as Ile and Phe expressed well in yeast and were capable of binding CO, indicative of proper folding, these mutant enzymes were devoid of any hydroxylase activity for EA or 1β(OH)EA.

EAH-S368A and EAH-S368T possess a K_m for the EA substrate that is similar to that of the wild-type enzyme, yet have a significantly higher K_m for 1β(OH)EA, suggesting that Ser[368] may be more instrumental for the second hydroxylation step rather than the first. Additional mutations at Ser[368] provided support for this notion. Both EAH-S368C and EAH-S368V readily catalyzed the biosynthesis of 1β(OH)EA without the generation of any capsidiol when incubated over a wide range of EA concentrations (Fig. 5). Interestingly, the EAH-S368C mutant produced 1β(OH)EA with a catalytic efficiency ~30% that of the wild-type enzyme and only a very negligible amount of EA-1-one (Table II). In contrast, the EAH-S368V mutant produced significant and approximately equal amounts of 1β(OH)EA, 2β(OH)EA, and 3β(OH)EA; a small amount of 3α(OH)EA; another unidentified monohydroxylated compound accounting for 7% of the total products (presumed to be 2α(OH)EA based on retention time and MS); and EA-3-one and EA-1-one at 1.5% (Fig. 6 and Scheme 2). Control microsomes (microsomes from yeast harboring an expression vector not engineered with any EAH gene constructs) were not able to metabolize 1β(OH)EA, but did exhibit a very minor activity (4.6% of that associated with EAH-S368V) for conversion of 3α(OH)EA to the corresponding ketone (data not shown). Overall, the catalytic efficiency of EAH-S368V for the turnover of EA to 1β(OH)EA was slightly superior to the ability of the wild-type enzyme to convert EA to capsidiol (Table II). However, when the biosynthetic rates for all the monohydroxylated and ketone reaction products are taken into account, EAH-S368V exhibited a turnover rate for EA twice that of the wild-type enzyme.

Ile[486] within SRS-6 was also chosen for mutagenesis because this position exhibits significant variability between other members of the CYP71D subfamily, and the spatial location of its R group is oriented into the active site based on molecular modeling (Fig. 4). Mutation of Ile[486] to Ala in EAH also caused a significant reduction in the successive hydroxylation of EA to capsidiol (Fig. 7 and Table II). The EAH-I486A mutant enzyme turned over EA to the monohydroxylated intermediate 1β(OH)EA at approximately one-half the rate of the wild-type enzyme, but produced only negligible amounts of capsidiol from EA. Because an accurate determination of the EA-to-capsidiol conversion was not possible, no kinetic constants for this reaction were calculated. However, the turnover rate for 1β(OH)EA to capsidiol by EAH-I486A had a 12-fold higher K_m and a 4-fold lower turnover rate compared to that of the wild-type enzyme (Table II).

DISCUSSION

The aim of this work was to determine whether successive hydroxylations of EA to capsidiol catalyzed by EAH occur with a preferred reaction order, and if so, if there are structural features of the EAH active site that can be associated with this specificity. Earlier work had demonstrated that EA is readily converted to capsidiol by EAH without the apparent release of any reaction intermediate(s) (14,41). This in turn prompted speculation that the successive hydroxylations might occur sequentially within a single catalytic cascade terminating with the release of only the dihydroxylated capsidiol product. The relatively large cavities described for the active site of several P450 enzymes (62,63) lent support to this notion. We therefore suggested that the initial monohydroxylated intermediate might not be released from EAH, but instead might be flipped and/or rotated within the active site in a manner to reposition the intermediate for the second hydroxylation event. The second hydroxylation event would then provide a trigger for product release. The present results clearly refute such speculation and provide strong kinetic evidence for independent and

stepwise hydroxylation of EA. EAH readily accepts and catalyzes the conversion of both monohydroxylated intermediates to capsidiol. However, although the turnover rate for 3α(OH)EA to capsidiol is comparable with that for the native hydrocarbon substrate EA, the relative efficiency for 1β(OH)EA conversion is 10-fold greater (Table I). The latter is largely accounted for by a much lower K_m for 1β(OH)EA. The accumulation of 1β(OH)EA in reactions initiated with concentrations of EA exceeding 20 μM also clearly demonstrates a specific reaction pathway. When EA concentrations are below 20 μM, EA must be converted first to 1β(OH)EA, which is released but rapidly recaptured and converted to the dihydroxylated product. At concentrations exceeding 20 μM (the approximate K_m for EA), EA effectively competes with released 1β(OH)EA for substrate-binding sites. Hence, 1β(OH)EA accumulates in direct proportion to the EA concentration.

The successive hydroxylation activity of EAH exhibits similarities and differences relative to other well characterized multifunctional P450 enzymes. For example, CYP27A1 catalyzes the successive hydroxylation of vitamin D$_3$ (64) and cholesterol (65). Based on the time-dependent appearance of multiple reaction products during *in vitro* reactions, Sawada *et al.* (64) concluded that CYP27A1 initially catalyzes hydroxylation at C-25 of vitamin D$_3$, followed by a second hydroxylation at C-24, C-1, or C-26, yielding a complex mixture of a single monohydroxylated product and three or more dihydroxylated ones. No C-1 or C-24 monohydroxylation products were observed, nor products with more than two inserted hydroxyls. Consistent with this complex reaction product profile, the K_m for the C-25 monohydroxylated intermediate is equal to that for the original substrate, but the apparent reaction velocity for the successive hydroxylation is only one-tenth that of the initial hydroxylation event. P450$_{11\beta}$ (66) and P450$_{17\alpha}$ lyase (67) are likewise P450 enzymes catalyzing successive hydroxylation reactions in aldosterone and androgen metabolism, respectively, that generate mono- and dihydroxylated reaction mixtures. Using rapid quench methods, rate constants for the initial hydroxylation step were shown to be ~10-fold greater than the rate constants for the second hydroxylation step, and the dissociation rates of the monohydroxylated intermediates were also competitive with the rate constants for the second hydroxylation step, altogether consistent with the release and accumulation of monohydroxylated intermediates over time. In light of these reports and the current results, our initial observation of complete conversion of EA to a single dihydroxylated product without release of monohydroxylated intermediate (14) can now be attributed to the greater affinity and faster turnover rate of EAH for the monohydroxylated intermediate than for the initial EA substrate.

Previous site-directed mutagenesis studies and the three-dimensional structure of mammalian P450 2C5 (36) provided important frameworks for targeting active-site residues that might play a role in the successive hydroxylation specificity of EAH (68,69). Using only those sequence regions that map to the active-site cavity of 2C5 and correspond to SRS-5 and SRS-6 (50), sequence alignment of select CYP71D family members revealed that the positions corresponding to amino acids 368 and 486 in EAH are particularly variable (Fig. 4). In fact, previous studies had already documented the functional significance of this variability. Mutagenesis of the position equivalent to amino acid 368 in several members of the CYP2B subfamily was shown to affect the regiospecific hydroxylation of steroids (52,53). The same position was also reported to play a role in substrate recognition for CYP2A5 (54) and CYP3A4 (55). Swapping this region between two highly homologous plant P450 enzymes, limonene 6-hydroxylase and limonene 3-hydroxylase, followed by reciprocal site-directed mutagenesis, demonstrated that the corresponding position also contributes to the regiospecificity of monoterpene hydroxylation. Exchange of Phe[363] with Ile changes the regiospecificity of limonene 6-hydroxylase (CYP71D18) from hydroxylating limonene at C-6 to C-3, but the reciprocal mutation, I363F, completely inactivates limonene 3-hydroxylase activity (56). A similar modification of the corresponding site (position 371)

in cinnamate hydroxylase (CYP73A1), another plant-specific P450 family, from Ile to Phe leads to a dramatic decrease in substrate binding and enzymatic activity, but without a major perturbation of protein folding (57).

The position corresponding to amino acid 486 in SRS-6 of EAH has also been extensively evaluated in mammalian hydroxylases. For instance, exchange of Gly[478] of CYP2B1 with larger hydrophobic amino acids (Ala, Val, Ile, and Leu) alters the stereospecific hydroxylation of androstenedione (58,59). In contrast, substitution of Phe for Ile at position 479 of CYP3A4 alters the regiospecific hydroxylation of 7-hexylcoumarin (60). Similarly, substitution of smaller hydrophobic amino acids (Ala, Val, and Leu) for Phe[494] in CYP94A2 also alters the regiospecificity of lauric acid hydroxylation (61). Finally, docking putative substrates into molecular models of four phenyl propanoid metabolism P450 enzymes from *Arabidopsis thaliana* (CYP84A1, CYP75B1, CYP98A3, and CYP73A5) was used to map substrate contact points to positions equivalent to amino acids 368 and 486 (51), but these have yet to be functionally confirmed by site-directed mutagenesis studies.

This work, summarized in Table III, demonstrates that positions 368 and 486 in EAH are both critical for regulating successive hydroxylation reactions as well as dictating regio-and stereospecificity. Substitution of Cys for Ser at position 368 completely abolished the capacity of EAH to generate capsidiol from either EA or 1β(OH)EA, yet the initial hydroxylation reaction of EA to 1β(OH)EA was preserved. Position 486 likewise is critical for the successive hydroxylation reaction. Although the EAH-I486A mutant readily catalyzed the biosynthesis of 1β(OH)EA from EA, it was severely compromised for capsidiol biosynthesis. The latter limitation was in fact correlated with a significant reduction in the binding affinity for the monohydroxylated intermediate.

The diversity of hydroxylated products generated by the EAH-S368V mutant underscores its importance in controlling stereo- and regiospecific hydroxylation. Although, like EAH-I486A, this mutant is severely compromised in its ability to convert 1β(OH)EA to capsidiol, it has a total activity 2-fold greater than that of the wild-type enzyme and generates at least five novel hydroxylation products (Fig. 6). These new products represent unique stereospecific products (3β(OH)EA), regiospecific isomers (2α(OH)EA and 2β(OH)EA), and novel successive hydroxylation products (EA-1-one and EA-3-one) that must arise from multiple hydroxylation reactions at C-1 and C-3, respectively (Scheme 2).

Substrate docking experiments using the EAH homology model provide a basis to rationalize the catalytic specificities of EAH and the various Ser[368] and Ile[486] mutations (Fig. 8). Multiple docking solutions for EA as ligand cluster around two distinct binding modes in which the plane of the bicyclic ring is rotated by ~180°. In binding mode A (Fig. 8*A*), the β-face of EA is directed toward the heme center, placing C-1 in position for hydroxylation to produce 1β(OH)EA. In binding mode B (Fig. 8*B*), C-3 is now poised for hydroxylation on the α-face leading to 3α(OH)EA. It is apparent from these binding models that the α-face is more hindered, given the methyl group on C-4. Therefore, one might expect that hydroxylation on the β-face may proceed faster.

Docking solutions using 1β(OH)EA as ligand cluster around a single binding mode, placing the β-hydroxy in the vicinity of Ser[368] for a potential hydrogen bonding interaction (Fig. 8*C*). Docking solutions for the 3α(OH)EA ligand produced a single nonproductive binding mode that directs the 3α-hydroxy group toward the heme center and C-1 away (data not shown). A compelling explanation for the greater catalytic efficiency of EAH for 1β(OH)EA than for 3α(OH)EA is that the hydroxyl group of Ser[368] anchors the 1β(OH)EA intermediate via a hydrogen bonding network (70) in a proper orientation for the second hydroxylation event. The EAH-S368A mutant may retain successive hydroxylation activity because it

accommodates an additional water molecule in the active-site pocket along with the monohydroxylated intermediate, and this water molecule complements the missing hydroxyl function of the Ser or Thr side chain. Confirmation of a hydrogen bonding network or the presence of an additional water molecule in the active site of EAH-S368A will be difficult without direct structural information on the EAH enzyme complexed with substrate analogs (62,63,70,71).

In summary, this work has established a preferred, kinetically discriminated reaction order for the successive hydroxylation of EA by EAH and demonstrated that successive hydroxylation shares important parallels with current models for how regio-and stereospecificity arise in cytochrome P450 enzymes. Sequence alignments of P450 enzymes, especially those representing the SRS regions (50), active-site residues (69), and those alignments between highly homologous but functionally distinct enzymes (56), have proven extremely useful in identifying structural features and amino acids contributing to such specificities of these enzymes. Elucidation of such specificities in the successive hydroxylation reactions of P450 enzymes such as EAH should also benefit from this comparative type of approach.

Supplementary Material

Refer to Web version on PubMed Central for supplementary material.

Acknowledgments

References

1. Stevens, KL. Isopentenoids in Plants. Marcel Dekker, Inc; New York: 1984. p. 63-80.

2. Kessler A, Baldwin IT. Science 2001;291:2141–2144. [PubMed: 11251117]

3. Gibson RW, Pickett JA. Nature 1983;302:608–609.

4. Chappell J. Plant Physiol 1995;107:1–6. [PubMed: 12228337]

5. Stoessl A, Stothers JB, Ward EWB. Phytochemistry 1976;15:855–873.

6. Stoessl A, Unwin CH, Ward EWB. Phytopathology 1973;63:1225–1231.

7. Ward EWB, Unwin CH, Stoessl A. Phytopathology 1973;63:1537–1538.

8. Guedes MEM, Kuc J, Hammerschmidt R, Bostock R. Phytochemistry 1982;21:2987–2988.

9. Watson DG, Rycroft DS, Freer IM, Brooks CJW. Phytochemistry 1985;24:2195–2200.

10. Chappell J, Nable R, Fleming P, Andersen RA, Burton HR. Phytochemistry 1987;26:2259–2260.

11. Stoessl A, Unwin CH, Ward EWB. Phytopathol Z 1972;74:141–152.

12. Vögeli U, Chappell J. Plant Physiol 1988;88:1291–1296. [PubMed: 16666457]

13. Facchini PJ, Chappell J. Proc Natl Acad Sci U S A 1992;89:11088–11092. [PubMed: 1438319]

14. Ralston L, Kwon ST, Schoenbeck M, Ralston J, Schenk DJ, Coates RM, Chappell J. Arch Biochem Biophys 2001;393:222–235. [PubMed: 11556809]

15. Lupien S, Karp F, Wildung M, Croteau R. Arch Biochem Biophys 1999;368:181–192. [PubMed: 10415126]

16. Wüst M, Little DB, Schalk M, Croteau R. Arch Biochem Biophys 2001;387:125–136. [PubMed: 11368174]

17. Teutsch HG, Hasenfratz MP, Lesot A, Stoltz C, Garnier JM, Jeltsch JM, Durst F, Werck-Reichhart D. Proc Natl Acad Sci U S A 1993;90:4102–4106. [PubMed: 8097885]

18. Meyer K, Cusumano JC, Somerville C, Chapple C. Proc Natl Acad Sci U S A 1996;93:6869–6874. [PubMed: 8692910]

19. Humphreys JM, Hemm MR, Chapple C. Proc Natl Acad Sci U S A 1999;96:10045–10050. [PubMed: 10468559]

20. Schoendorf A, Rithner CD, Williams RM, Croteau RB. Proc Natl Acad Sci U S A 2001;98:1501–1506. [PubMed: 11171980]

21. Jennewein S, Rithner CD, Williams RM, Croteau RB. Proc Natl Acad Sci U S A 2001;98:13595–13600. [PubMed: 11707604]

22. Jennewein S, Rithner CD, Williams RM, Croteau R. Arch Biochem Biophys 2003;413:262–270. [PubMed: 12729625]

23. Frey M, Chomet P, Glawischnig E, Stettner C, Grun S, Winklmair A, Eisenreich W, Bacher A, Meeley RB, Briggs SP, Simcox K, Gierl A. Science 1997;277:696–699. [PubMed: 9235894]

24. Nomura T, Ishihara A, Imaishi H, Endo TR, Ohkawa H, Iwamura H. Mol Genet Genomics 2002;267:210–217. [PubMed: 11976964]

25. Szekeres M, Nemeth K, Koncz-Kalman Z, Mathur J, Kauschmann A, Altmann T, Redei GP, Nagy F, Schell J, Koncz C. Cell 1996;85:171–182. [PubMed: 8612270]

26. Choe S, Dilkes BP, Fujioka S, Takatsuto S, Sakurai A, Feldmann KA. Plant Cell 1998;10:231–243. [PubMed: 9490746]

27. Koch BM, Sibbesen O, Halkier BA, Svendsen I, Moller BL. Arch Biochem Biophys 1995;323:177–186. [PubMed: 7487064]

28. Kaltenbach M, Schroder G, Schmelzer E, Lutz V, Schroder J. Plant J 1999;19:183–193. [PubMed: 10476065]

29. Menting J, Scopes RK, Stevenson TW. Plant Physiol 1994;106:633–642. [PubMed: 12232356]

30. Xu YL, Li L, Wu K, Peeters AJ, Gage DA, Zeevaart JA. Proc Natl Acad Sci U S A 1995;92:6640–6644. [PubMed: 7604047]

31. Phillips AL, Ward DA, Uknes S, Appleford NE, Lange T, Huttly AK, Gaskin P, Graebe JE, Hedden P. Plant Physiol 1995;108:1049–1057. [PubMed: 7630935]

32. Helliwell CA, Poole A, Peacock WJ, Dennis ES. Plant Physiol 1999;119:507–510. [PubMed: 9952446]

33. Helliwell CA, Chandler PM, Poole A, Dennis ES, Peacock WJ. Proc Natl Acad Sci U S A 2001;98:2065–2070. [PubMed: 11172076]

34. Watson DG, Baker FC, Brooks CJW. Biochem Soc Trans 1983;11:589–590.

35. Whitehead IM, Threlfall DR, Ewing DF. Phytochemistry 1989;28:775–779.

36. Williams PA, Cosme J, Sridhar V, Johnson EF, McRee DE. Mol Cell 2000;5:121–131. [PubMed: 10678174]

37. Zhao Y, Schenk DJ, Takahashi S, Chappell J, Coates RM. J Org Chem 2004;69:7428–7435. [PubMed: 15497966]

38. Rising KA, Starks CM, Noel JP, Chappell J. J Am Chem Soc 2000;122:1861–1866.

39. Pompon D, Louerat B, Bronine A, Urban P. Methods Enzymol 1996;272:51–64. [PubMed: 8791762]

40. Urban P, Mignotte C, Kazmaier M, Delorme F, Pompon D. J Biol Chem 1997;272:19176–19186. [PubMed: 9235908]

41. Greenhagen BT, Griggs P, Takahashi S, Ralston L, Chappell J. Arch Biochem Biophys 2003;409:385–394. [PubMed: 12504906]

42. Omura T, Sato R. J Biol Chem 1964;239:2370–2378. [PubMed: 14209971]

43. Marti-Renom MA, Stuart A, Fiser A, Sánchez R, Melo F, Sali A. Annu Rev Biophys Biomol Struct 2000;29:291–325. [PubMed: 10940251]

44. Sali A, Blundell TL. J Mol Biol 1993;234:779–815. [PubMed: 8254673]

45. Fiser A, Do RK, Sali A. Protein Sci 2000;9:1753–1773. [PubMed: 11045621]

46. Jones G, Willett P, Glen RC. J Mol Biol 1995;245:43–53. [PubMed: 7823319]

47. Jones G, Willett P, Glen RC, Leach AR, Taylor R. J Mol Biol 1997;267:727–748. [PubMed: 9126849]

48. Nissink JWM, Murray C, Hartshorn M, Verdonk ML, Cole JC, Taylor R. Proteins 2002;49:457–471. [PubMed: 12402356]

49. Verdonk ML, Cole JC, Hartshorn MJ, Murray CW, Taylor RD. Proteins 2003;52:609–623. [PubMed: 12910460]

50. Gotoh O. J Biol Chem 1992;267:83–90. [PubMed: 1730627]

51. Rupasinghe S, Baudry J, Schuler MA. Protein Eng 2003;16:721–731. [PubMed: 14600201]

52. He Y, Luo Z, Klekotka PA, Burnett VL, Halpert JR. Biochemistry 1994;33:4419–4424. [PubMed: 8155660]

53. Hasler JA, Harlow GR, Szklarz GD, John GH, Kedzie KM, Burnett VL, He YA, Kaminsky LS, Halpert JR. Mol Pharmacol 1994;46:338–345. [PubMed: 8078495]

54. Pelkonen P, Lang MA, Negishi M, Wild CP, Juvonen RO. Chem Res Toxicol 1997;10:85–90. [PubMed: 9074807]

55. He YA, He YQ, Szklarz GD, Halpert JR. Biochemistry 1997;22:8831–8839. [PubMed: 9220969]

56. Schalk M, Croteau R. Proc Natl Acad Sci U S A 2000;97:11948–11953. [PubMed: 11050228]

57. Schoch GA, Attias R, Le Ret M, Werck-Reichhart D. Eur J Biochem 2003;270:3684–3695. [PubMed: 12950252]

58. Kedzie KM, Balfour CA, Escobar GY, Grimm SW, He YA, Pepperl DJ, Regan JW, Stevens JC, Halpert JR. J Biol Chem 1991;266:22515–22521. [PubMed: 1718996]

59. He YA, Balfour CA, Kedzie KM, Halpert JR. Biochemistry 1992;31:9220–9226. [PubMed: 1390709]

60. Khan KK, Halpert JR. Arch Biochem Biophys 2000;373:335–345. [PubMed: 10620357]

61. Kahn RA, Le Bouquin R, Pinot F, Benveniste I, Durst F. Arch Biochem Biophys 2001;15:180–187. [PubMed: 11437349]

62. Williams PA, Cosme J, Ward A, Angove HC, Matak VD, Jhoti H. Nature 2003;424:464–468. [PubMed: 12861225]

63. Williams PA, Cosme J, Vinkovic DM, Ward A, Angove HC, Day PJ, Vonrhein C, Tickle IJ, Jhoti H. Science 2004;305:683–686. [PubMed: 15256616]

64. Sawada N, Sakaki T, Ohta M, Inouye K. Biochem Biophys Res Commun 2000;273:977–984. [PubMed: 10891358]

65. Pikuleva I, Javitt NB. Arch Biochem Biophys 2003;420:35–39. [PubMed: 14622972]

66. Imai T, Yamazaki T, Kominami S. Biochemistry 1998;37:8097–8104. [PubMed: 9609704]

67. Yamazaki T, Ohno T, Sakaki T, Akiyoshi-Shibata M, Yabusaki Y, Imai T, Kominami S. Biochemistry 1998;37:2800–2806. [PubMed: 9485431]

68. Lewis DFV. J Inorg Biochem 2002;91:502–514. [PubMed: 12237218]

69. Kumar S, Scott EE, Liu H, Halpert JR. J Biol Chem 2003;278:17178–17184. [PubMed: 12609983]

70. Wester MR, Johnson EF, Marques-Soares C, Dijols S, Dansette PM, Mansuy D, Stout CD. Biochemistry 2003;42:9335–9345. [PubMed: 12899620]

71. Scott EE, White MA, He YA, Johnson EF, Stout CD, Halpert JR. J Biol Chem 2004;279:27294–27301. [PubMed: 15100217]

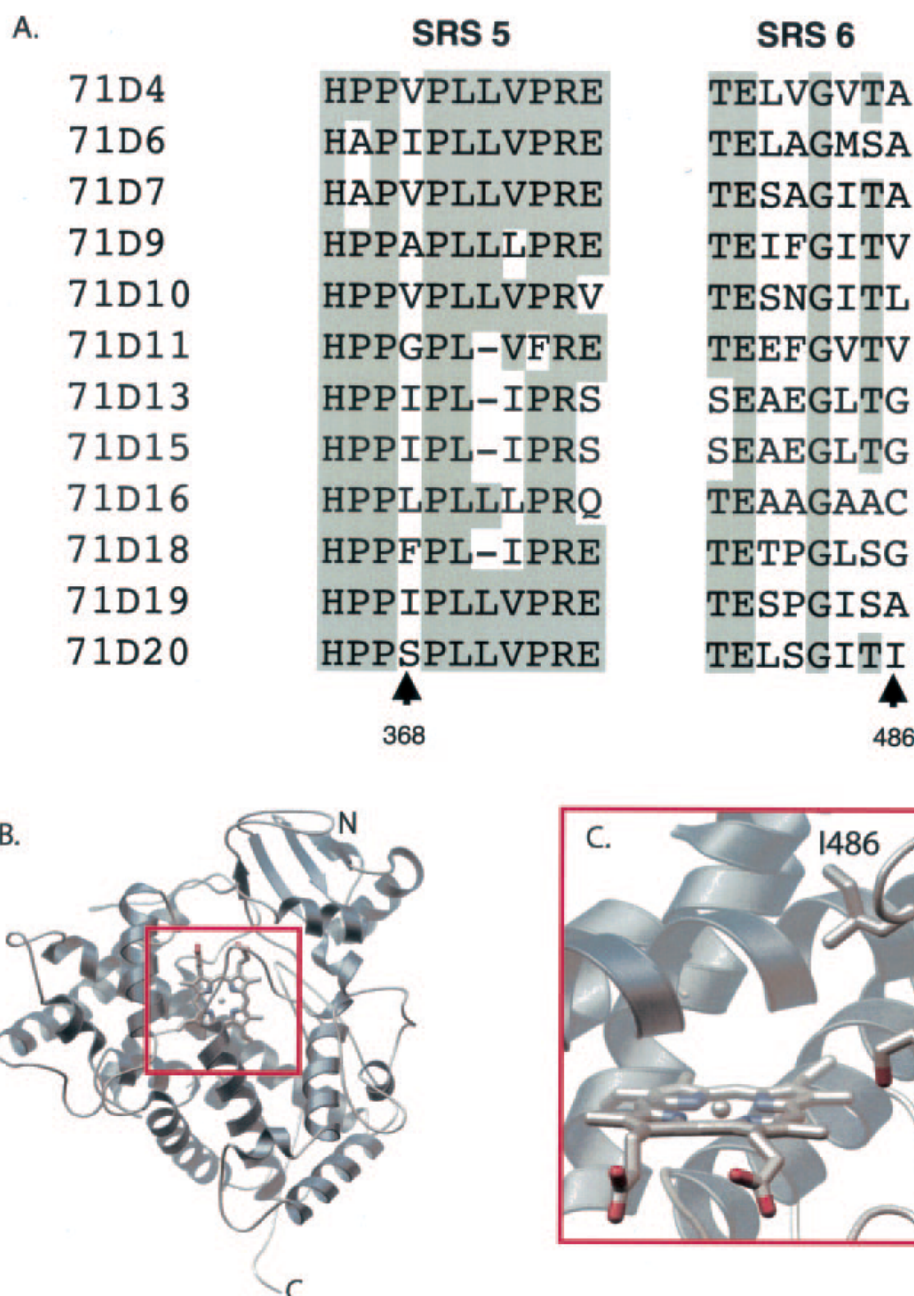72. Wang E, Wang R, DeParasis J, Loughrin JH, Gan S, Wagner GJ. Nat Biotechnol 2001;19:371–374. [PubMed: 11283597]
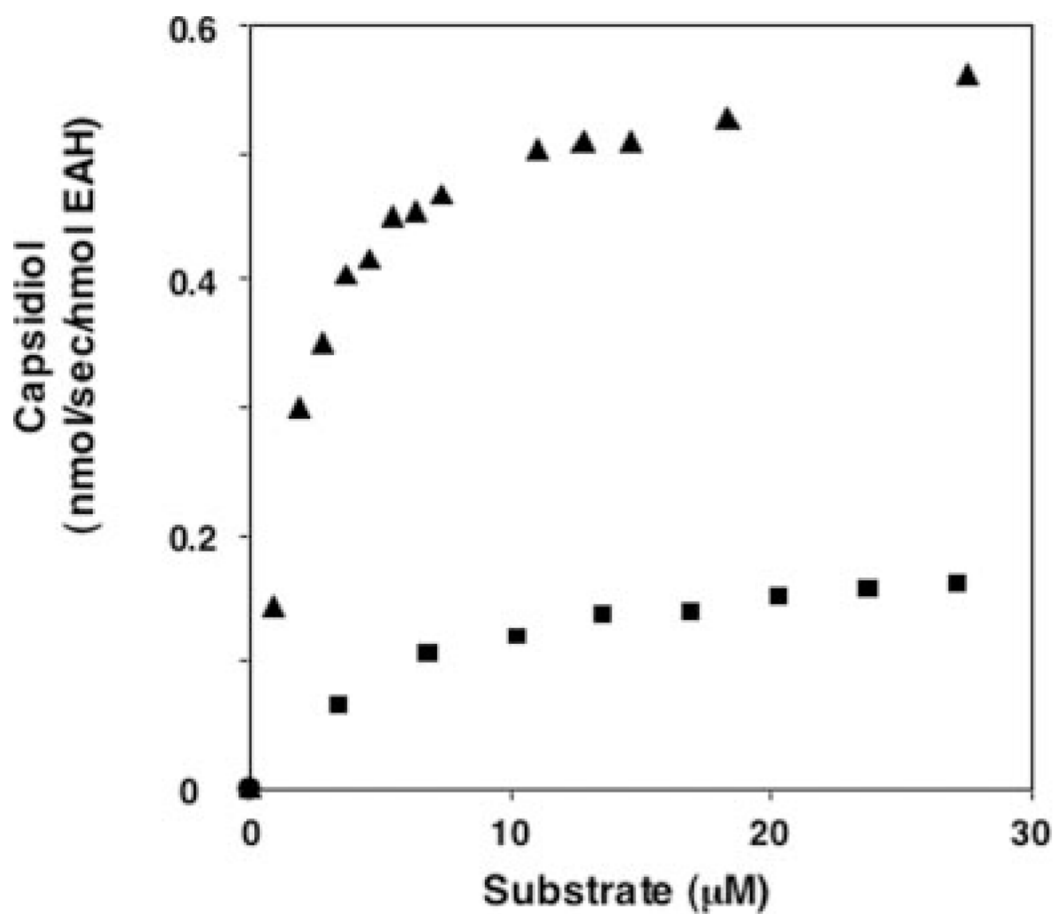
Fig. 1. Concentration-dependent conversion of putative monohydroxylated intermediates to capsidiol by EAH

$3\alpha(OH)EA$ (■), $1\beta(OH)EA$ (▲), or both are potential intermediates in the catalytic conversion of the natural bicyclic hydrocarbon substrate EA to capsidiol. EAH was incubated at the indicated concentrations of substrate for 1 ($1\beta(OH)EA$) or 5 ($3\alpha(OH)EA$) min before identifying and quantifying capsidiol accumulation by GC/MS.
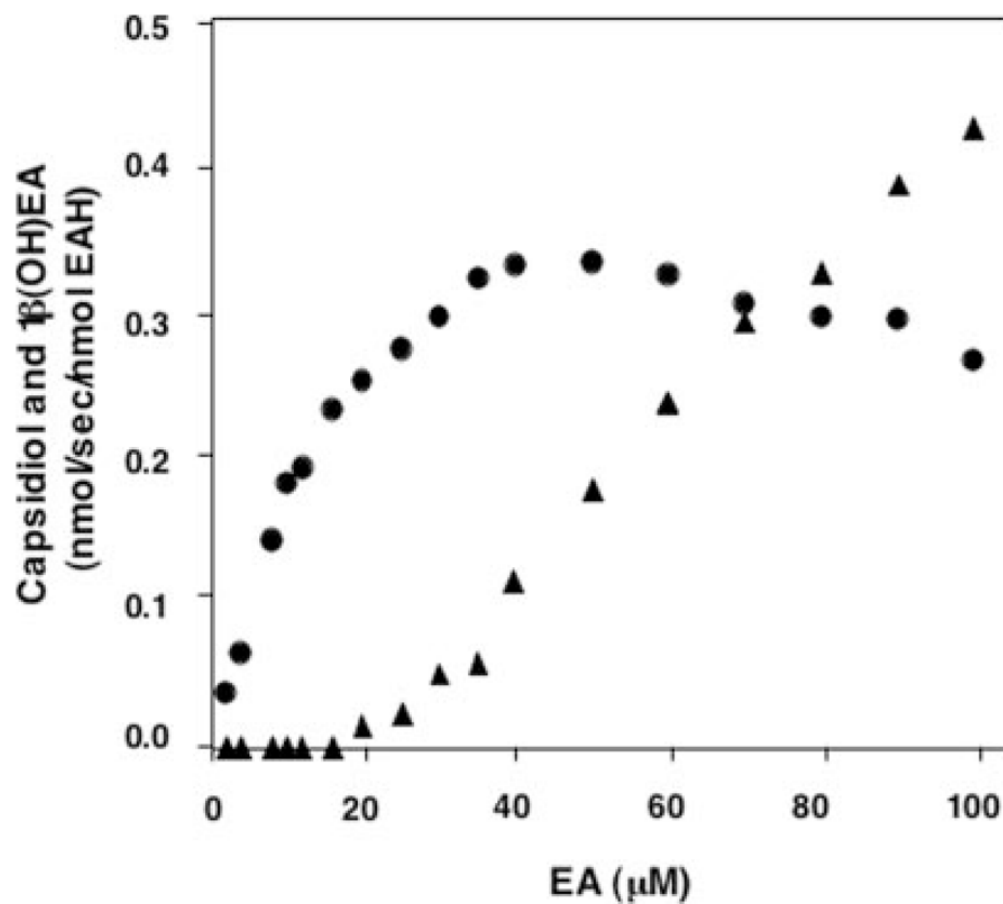
Fig. 2. Concentration-dependent conversion of EA to capsidiol by EAH
EAH was incubated at the indicated concentrations of EA for 2 min before profiling the reaction products by GC/MS. Capsidiol (●) and 1β(OH)EA (▲) were the only NADPH-dependent reaction products detected.
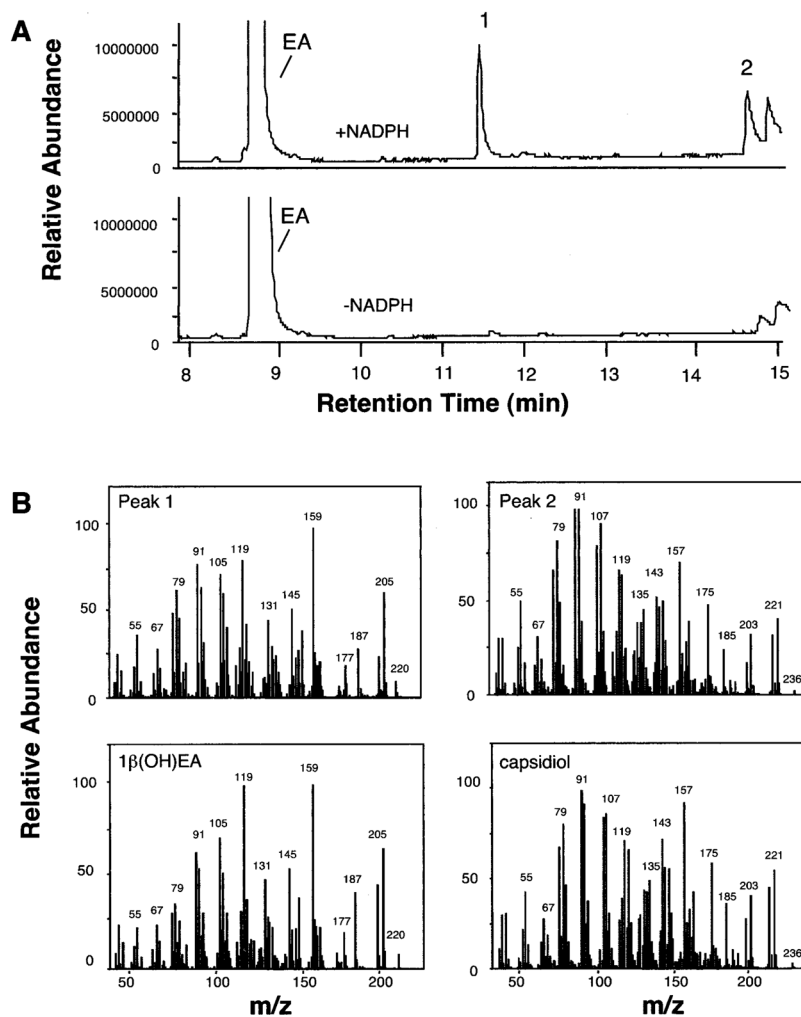
Fig. 3. GC and MS profiles for the reaction products generated by EAH incubated with EA
Shown are total ion chromatograms for reaction products generated by EAH in the presence and absence of NADPH (*A*) and mass spectrum matches for peaks 1 and 2 to authentic standards of 1β(OH)EA and capsidiol (*B*).

A.

|	**SRS 5**	**SRS 6**
71D4	HPPVPLLVPRE	TELVGVTA
71D6	HAPIPLLVPRE	TELAGMSA
71D7	HAPVPLLVPRE	TESAGITA
71D9	HPPAPLLLPRE	TEIFGITV
71D10	HPPVPLLVPRV	TESNGITL
71D11	HPPGPL-VFRE	TEEFGVTV
71D13	HPPIPL-IPRS	SEAEGLTG
71D15	HPPIPL-IPRS	SEAEGLTG
71D16	HPPLPLLLPRQ	TEAAGAAC
71D18	HPPFPL-IPRE	TETPGLSG
71D19	HPPIPLLVPRE	TESPGISA
71D20	HPPSPLLVPRE	TELSGITI

368 486

Fig. 4. Associating amino acids with the regio- and stereospecificity of EAH by amino acid sequence alignment and protein modeling
Shown is a sequence alignment for select members of the CYP71D subfamily corresponding to SRS-5 and SRS-6 (50), with identical amino acids *shaded* (*A*). GenBank™/EBI accession numbers are as follows: CYP71D4 (AJ296346), CYP71D6 (U48434), CYP71D7 (U48435), CYP71D9 (Y10490), CYP71D10 (AF022459), CYP71D11 (AF000403), CYP71D13 (AF124816), CYP71D15 (AF124817), CYP71D16 (AF166332), CYP71D18 (AF124815), CYP71D19 (AF122821), and CYP71D20 (EAH; AF368376). Several of the CYP71D subfamily members have not been functionally characterized, whereas CYP71D13 and CYP71D15 code for (4*S*)-limonene 3-hydroxylase (15), CYP71D18 for (4*S*)-limonene 6-hydroxylase (15), CYP71D16 for a diterpene hydroxylase (72), and CYP71D20 for EAH

(14). A homology model of EAH was generated using the mammalian P450 2C5 protein (Protein Data Bank code 1DT6) (36) as described under "Experimental Procedures" and is shown here as a ribbon diagram (*B*). A close-up is shown of the active-site model of EAH showing the spatial location of Ser[368] and Ile[486] relative to the heme reaction center (*C*).
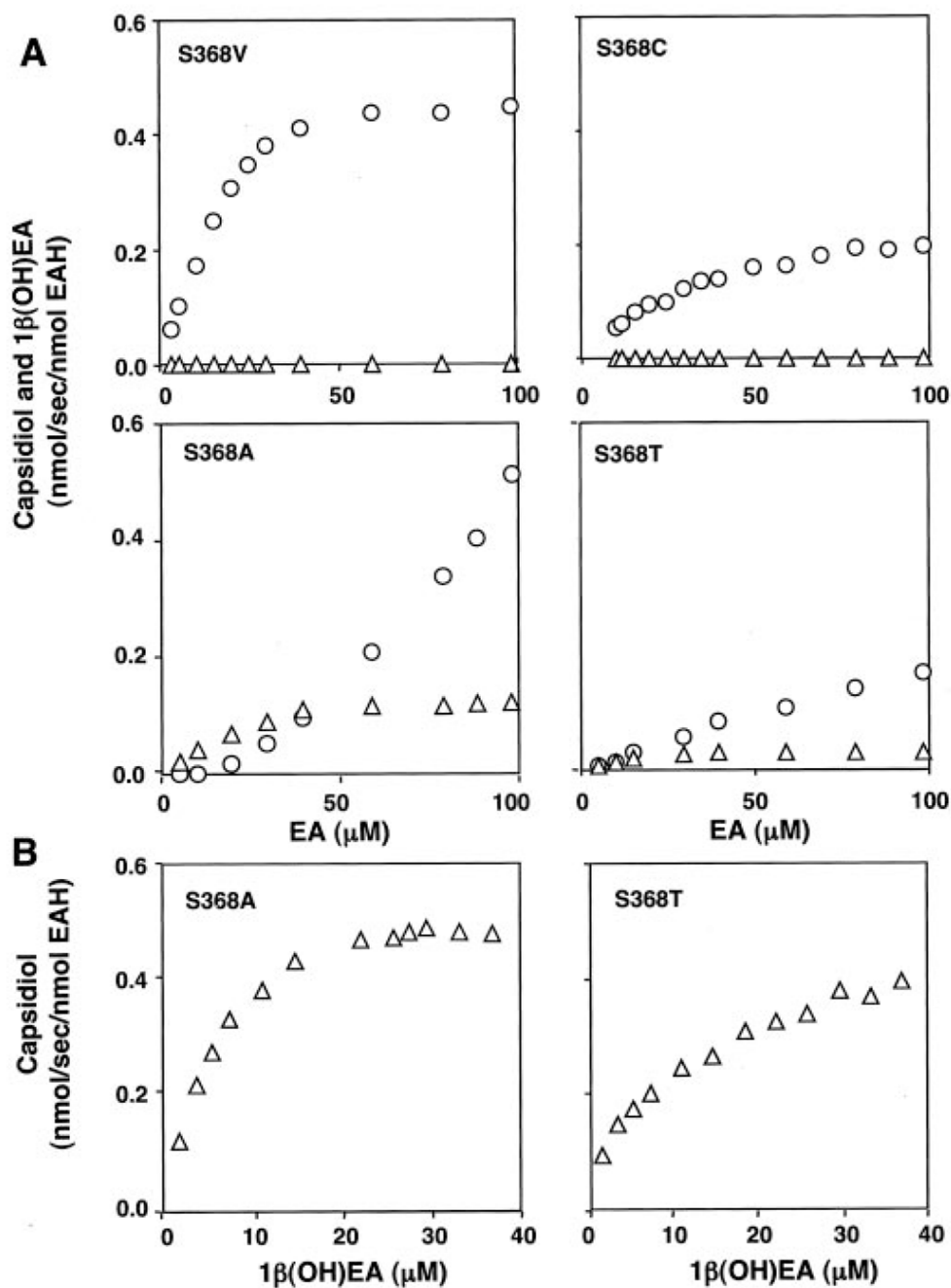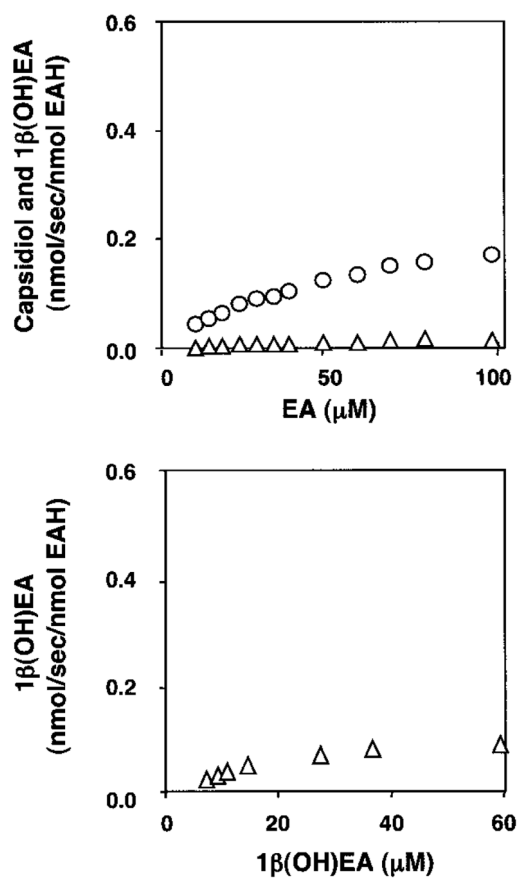
Fig. 5. Substrate-dependent activities of the EAH Ser[368] mutants
Site-specific mutations corresponding to Ser[368] were introduced into the EAH gene as described under "Experimental Procedures"; the mutant genes were expressed in yeast; and yeast microsomes were prepared as the source for each mutant P450 enzyme. CO difference spectroscopy was used to qualify and normalize the amount of properly folded P450 enzyme used in the activity assays. Microsome preparations were incubated at the indicated concentrations of EA or 1β(OH)EA before profiling the reaction products by GC/MS. Except for the EAH-S368V mutant, which generated multiple reaction products, the only NADPH-dependent reaction products observed were capsidiol ($\triangle$) and 1β(OH)EA ($\circ$).
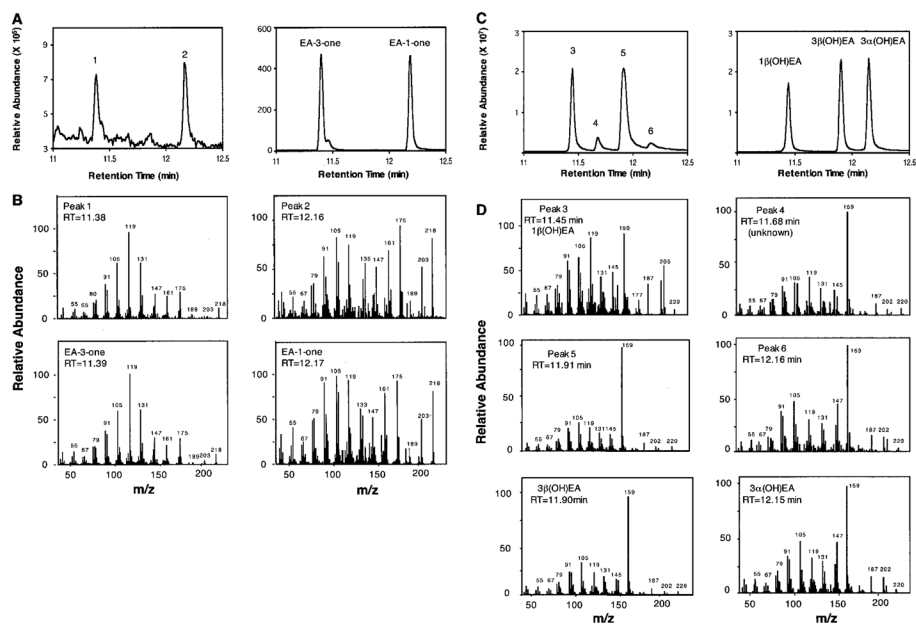
Fig. 6. Reaction product analysis of EAH-S368V incubated with EA
EAH-S368V was incubated with 40 μM EA, and the total reaction products were
fractionated by silica gel chromatography. Total ion chromatograms of the reaction products
eluted from the silica gel with 5% ethyl acetate in hexane (*A*, *left panel*) are compared with
those of authentic standards for EA-3-one and EA-1-one (*A*, *right panel*). Mass spectra for
peaks 1 and *2* are compared directly with those for the respective ketones (*B*). Total ion
chromatograms of reaction products sequentially eluted from the silica gel with 20% ethyl
acetate in hexane (*C*, *left panel*) are compared with those of authentic standards for
1β(OH)EA, 3α(OH)EA, and 3β(OH)EA (*C*, *right panel*). The mass spectrum for *peak 3*
matches that for 1β(OH)EA (*D*), shown previously in Fig. 3. The mass spectra for *peaks 5*
and *6* are compared directly with those for 3β(OH)EA and 3α(OH)EA (*D*). However, *peak 5*
resolves into two nearly equal sized peaks by chiral GC analysis (Supplemental Fig. 2), with
peak 5-1 corresponding to 3β(OH)EA and *peak 5-2* to 2β(OH)EA (as determined by NMR
analysis). *RT*, retention time.

Fig. 7. Substrate-dependent activities of the EAH-I486A mutant
The EAH-I486A mutation was created as described under "Experimental Procedures"; the mutant gene was expressed in yeast; and yeast microsomes were prepared as the source of the EAH-I486A enzyme. CO difference spectroscopy was used to qualify and normalize the amount of properly folded P450 enzyme used in the activity assays. Assays were incubated at the indicated concentrations of EA for 5 min (*upper panel*) or 1β(OH)EA for 1 min (*lower panel*) before profiling the reaction products by GC/MS. The only NADPH-dependent reaction products observed were capsidiol ($\triangle$) and 1β(OH)EA ($\circ$). Capsidiol levels were near the detection limits for reactions incubated with EA.
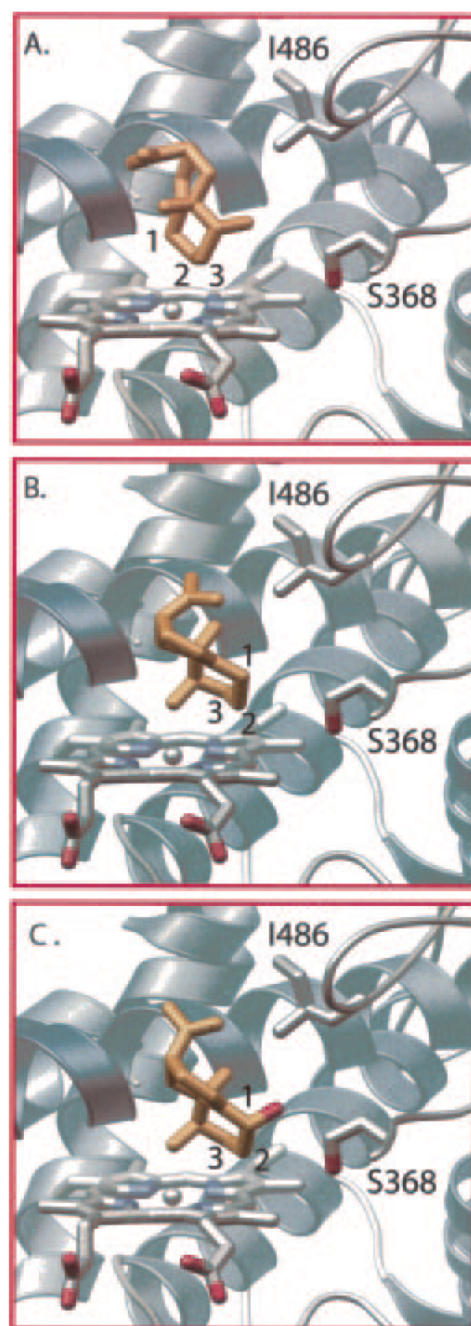
Fig. 8. Docking of EA and 1β(OH)EA into a modeled EAH active site
A homology model of EAH was created using the mammalian P450 2C5 (Protein Data Bank code 1DT6) as template and was used for docking experiments with EA and 1β(OH)EA ligands as described under "Experimental Procedures." Two distinct binding modes of EA that position the β-face of EA toward the heme center for oxidation at C-1 (*A*) or that place the α-face toward the heme center for C-3 oxidation (*B*) were predicted from docking experiments. A single binding mode for 1β(OH)EA (*C*) that poises C-3 near the heme center for oxidation was predicted. The β-hydroxy is directed toward the hydroxyl group of Ser[368] for possible hydrogen bonding interactions. Relevant carbon atoms are numbered, and important active-site residues are displayed and labeled.
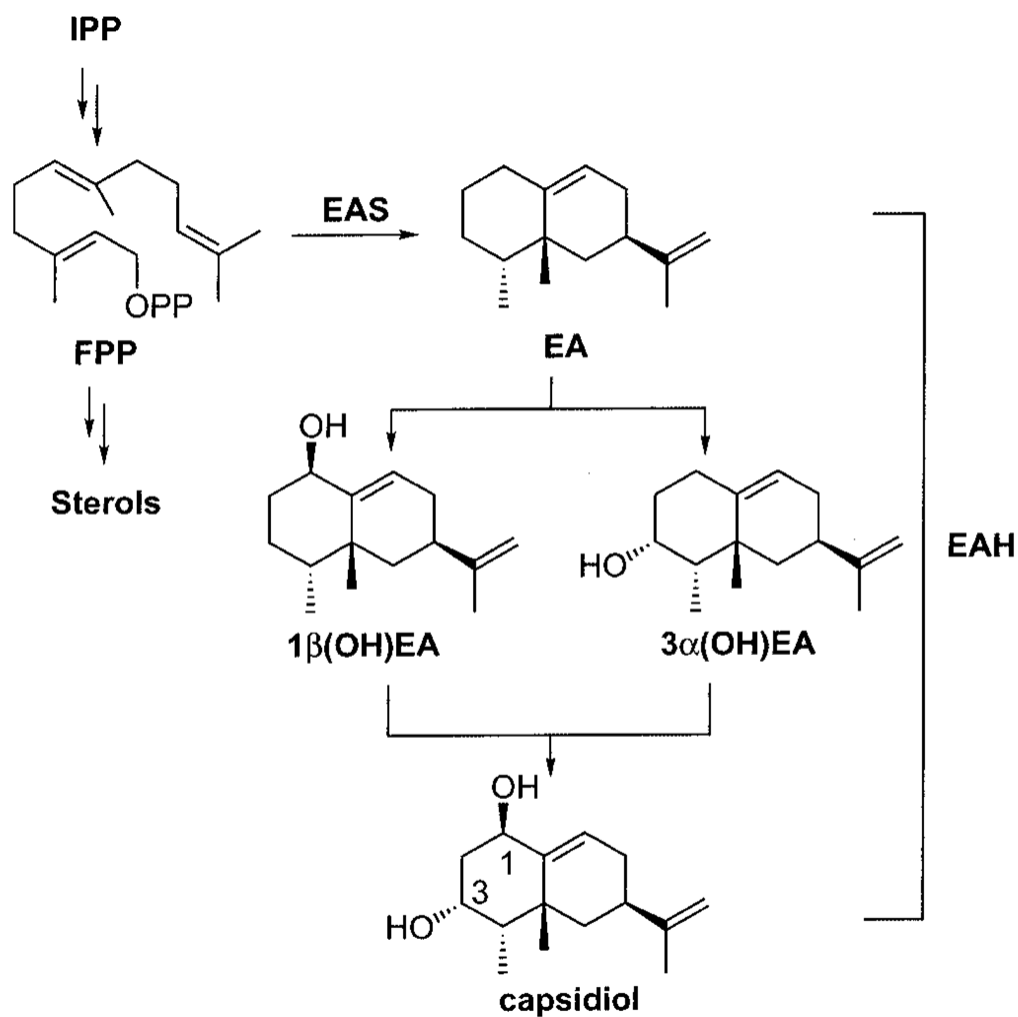
Scheme 1. Biosynthetic pathway for capsidiol in elicitor-treated *N. tabacum* cells
Farnesyl diphosphate (*FPP*) is diverted from the central mevalonate pathway via the action
of a sesquiterpene synthase (5-epiaristolochene synthase (*EAS*)) to generate EA. Subsequent
hydroxylations at C-1 and C-3 catalyzed by EAH yield capsidiol. A preferred hydroxylation
order had not been established previously. *IPP*, isopentenyl pyrophosphate; *OPP*,
pyrophosphate.
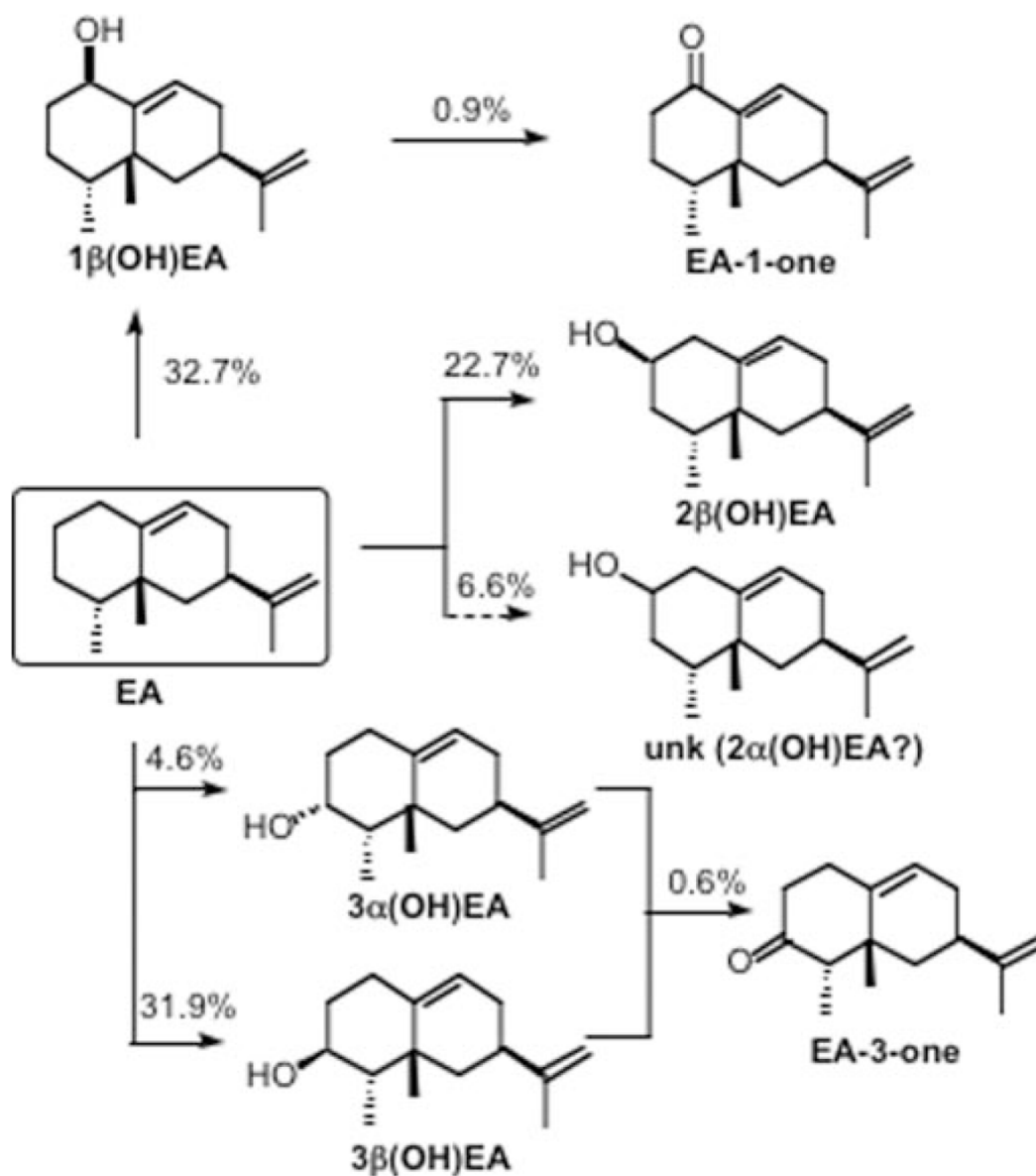
Scheme 2. Chemical rationalization for the reaction products generated by the EAH-S368V mutant

Solid arrows refer to reaction products identified by comparison with authentic standards or directly by NMR, whereas the *dashed arrow* refers to a reaction product structure inferred from GC retention times and MS profiles. The percentages denote the amount of a particular reaction product generated in a typical reaction assay. *unk*, unknown

Table I

Comparison of the EAH kinetic constants for its initial substrate (EA) and two possible monohydroxylated intermediates

Substrate	Product	K_m	k_{cat}	k_{cat}/K_m
		μM	s^{-1}	$s^{-1}/\mu M$
EA	CD	19.18 ± 2.90	0.493 ± 0.039	0.0257
3α(OH)EA	CD	6.38 ± 0.42	0.200 ± 0.004	0.0313
1β(OH)EA	CD	1.74 ± 0.08	0.582 ± 0.006	0.3344

Constants were calculated by nonlinear regression fits to the Michaelis-Menten equation using the data from Figs. 1 and 2. CD, capsidiol reaction product.

Table II

Comparison of the kinetic constants for EAH and several site-specific mutants for the initial substrate (EA) and the monohydroxylated intermediate 1β(OH)EA
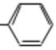
Enzyme	Substrate	Product	K_m	k_{cat}	k_{cat}/K_m
			μM	s^{-1}	$s^{-1}/\mu M$
Wild-type	EA	CD	19.18 ± 2.90	0.493 ± 0.039	0.0257
S368A	EA	CD	22.67 ± 4.00	0.154 ± 0.009	0.0068
S368T	EA	CD	15.18 ± 1.55	0.037 ± 0.001	0.0024
I486A	EA	CD	ND		
Wild-type	1β(OH)EA	CD	1.74 ± 0.08	0.582 ± 0.006	0.3344
S368A	1β(OH)EA	CD	6.20 ± 0.47	0.581 ± 0.012	0.0937
S368T	1β(OH)EA	CD	9.97 ± 1.14	0.482 ± 0.019	0.0483
S368C	1β(OH)EA	CD	NA		
S368V	1β(OH)EA	CD	NA		
I486A	1β(OH)EA	CD	21.24 ± 2.84	0.132 ± 0.008	0.0062
S368C	EA	1β(OH)EA	38.63 ± 2.64	0.278 ± 0.008	0.0072
S368V	EA	1β(OH)EA	16.72 ± 2.21	0.553 ± 0.025	0.0331
I486A	EA	1β(OH)EA	68.80 ± 4.04	0.293 ± 0.010	0.0043

Constants were calculated by nonlinear regression fits to the Michaelis-Menten equation using the data from Figs. 1, 2, and 5. CD, capsidiol reaction product; ND, not determined (enzyme activity too low to calculate kinetic parameters); NA, no activity.

Table III

Summary comparisons of mutations at Ser[368] and Ile[486] on the successive hydroxylation activity of EAH

Amino acid/ position	-R group	Reaction after feeding substrate		
		EA		1β(OH)EA
368A	-CH₃	++[1]		+++++[2]
368S (wt)	-CH₂OH	+++++[1]		+++++[2]
368C	-CH₂SH	+++[1]	No activity	No activity
368T	-CHCH₃ / OH	+[1]		++++[2]
368V	-CHCH₃ / CH₃	++++++[1]	No activity	No activity
368I	-CHCH₂CH₃ / CH₃	No activity	No activity	No activity
368F	-CH₂ ⬡	No activity	No activity	No activity
486A	-CH₃	+++[1]	No activity	+[2]
486I (wt)	-CHCH₂CH₃ / CH₃	+++++[1]		+++++[2]

[1] Calculated as percent of the wild-type k_{cat} of 0.493.

[2] Calculated as percent of the wild-type k_{cat} of 0.582.